

Scaling of Dynamical Decoupling for Spin Qubits

J. Medford¹, Ł. Cywiński², C. Barthel¹, C. M. Marcus¹, M. P. Hanson³, and A. C. Gossard³

¹*Department of Physics, Harvard University, Cambridge, Massachusetts 02138, USA*

²*Institute of Physics, Polish Academy of Sciences,
Al. Lotników 32/46, PL 02-668 Warszawa, Poland*

³*Materials Department, University of California, Santa Barbara, California 93106, USA*

(Dated: February 18, 2022)

We investigate scaling of coherence time, T_2 , with the number of π -pulses, n_π , in a singlet-triplet spin qubit using Carr-Purcell-Meiboom-Gill (CPMG) and concatenated dynamical decoupling (CDD) pulse sequences. For an even numbers of CPMG pulses, we find a power law, $T_2 \propto (n_\pi)^{\gamma_e}$, with $\gamma_e = 0.72 \pm 0.01$, essentially independent of the envelope function used to extract T_2 . From this surprisingly robust value, a power-law model of the noise spectrum of the environment, $S(\omega) \sim \omega^{-\beta}$, yields $\beta = \gamma_e/(1 - \gamma_e) = 2.6 \pm 0.1$. Model values for $T_2(n_\pi)$ using $\beta = 2.6$ for CPMG with both even and odd n_π up to 32 and CDD orders 3 through 6 compare very well with experiment.

PACS numbers:

A variety of solid state systems are emerging as effective platforms for studying decoherence and entanglement in controlled quantum systems [1–4]. Among them, quantum-dot-based spin qubits have recently achieved sufficient control and long coherence times [1, 2] that new information about the noise environment of the qubit can be extracted, complementing related work in nitrogen-vacancy centers in diamond [4], superconducting qubits [3], trapped ions [5], and neutral atoms [6].

Dynamical decoupling in the form of a sequence of π -pulses [7–10] functions as a high-pass filter, thus providing information about the spectral content of environmental noise [3–5, 11–14]. For spin qubits, the effectiveness of various decoupling schemes at mitigating dephasing due to nuclear bath dynamics has been well studied theoretically [15–19]. Much less is known about mitigating the effects of charge noise, which couples to the qubit via gate dependent exchange interaction and through spatially varying Overhauser fields [1]. When the decoherence time, T_2 , is short compared to the energy relaxation time, T_1 ,—which is the case in this study—both the envelope of the coherence decay as well as the dependence of T_2 on the number of π -pulses, n_π , depend on the spectral density of the environment, $S(\omega)$. Knowledge of $S(\omega)$ inferred from such measurements can in turn be used to design optimal decoupling sequences [5, 12, 20–22].

In this Letter, we investigate scaling of T_2 with the number of π -pulses for Carr-Purcell-Meiboom-Gill (CPMG) and concatenated dynamical decoupling (CDD) sequences in a GaAs two-electron singlet-triplet qubit [Fig. 1(a)]. The coherence envelope is reasonably well described by the form $\exp(-(\tau_D/T_2)^\alpha)$, where τ_D is the time during which π -pulses are applied [Fig. 2(b)]. It is difficult, however, to accurately determine α by directly fitting to this form. In contrast, we find that the scaling relation $T_2 \sim (n_\pi)^\gamma$ very accurately describes the data irrespective of the value of α used to extract T_2 . The resulting γ can then be related to α and other quanti-

ties of interest within specific noise models. For CPMG with even n_π , the scaling relation $T_2 \propto (n_\pi)^{\gamma_e}$ yields $\gamma_e = 0.72 \pm 0.01$, using T_2 values extracted using any α in the range 2 to 5. A model of dephasing due to a power-law spectrum of classical noise, $S(\omega) \sim \omega^{-\beta}$, leads to a scaling relation in the number of π -pulses, with the exponent of the power law, β , related to the scaling exponent by the simple relation $\beta = \gamma_e/(1 - \gamma_e)$. For the present experiment, $\gamma_e = 0.72$ thus yields $\beta = 2.6$. Further support for a power-law form for $S(\omega)$ is found by comparing experimental and theoretical dependences $T_2(n_\pi)$ for CPMG with both even and odd n_π as well as CDD pulse sequences. This model also gives the simple relation $\alpha = \beta + 1$ connecting the noise spectrum and the decoherence envelope exponent. The resulting value, $\alpha = 3.6 \pm 0.1$ is thus determined with considerably greater accuracy than can be obtained from direct fits to the coherence envelope data.

The lateral double quantum dot investigated was defined by Ti/Au depletion gates patterned using electron beam lithography on a GaAs/Al_{0.3}Ga_{0.7}As heterostructure with a two dimensional electron gas (density 2×10^{15}

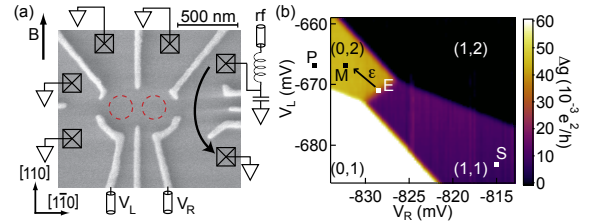


FIG. 1: (Color online) (a) Micrograph of lithographically identical device with dot locations depicted. Gate voltages, $V_{R(L)}$, set the charge occupancy of right (left) dot as well as the detuning of the qubit. An rf-sensor quantum dot is indicated on the right. (b) Double dot charge state mapped onto dc conductance change, Δg , with lettered pulse sequence gate voltages. Detuning axis is orthogonal to the (0,2)-(1,1) charge degeneracy through points E, S, and M.

m^{-2} , mobility $20 \text{ m}^2/\text{V s}$) 100 nm below the surface. Measurements were performed in a dilution refrigerator with an electron temperature $T_e \sim 150 \text{ mK}$. The double quantum dot is operated as a spin qubit by first depleting the quantum dots to the last two electrons, then manipulating the charge occupancy of the two dots with high bandwidth plunger gates V_L and V_R along a detuning axis ϵ [Fig. 1(b)]. In this work, the charge occupancy was manipulated between states $(0,2)$ and $(1,1)$, where (N_L, N_R) represent the charge in the left and right dots. Charge occupancy was determined by the conductance change, Δg , through a proximal sensor quantum dot, which in turn modulated the reflection coefficient of the radio-frequency (rf) readout circuit [23, 24].

The logical spin qubit subspace is spanned by the singlet ($S = (|\uparrow\downarrow\rangle - |\downarrow\uparrow\rangle)/\sqrt{2}$) and the $m = 0$ triplet ($T_0 = (|\uparrow\downarrow\rangle + |\downarrow\uparrow\rangle)/\sqrt{2}$) states of two electrons. The $m = \pm 1$ triplet states were split off by a 750 mT magnetic field applied in the plane of the electron gas, perpendicular to the dot connection axis. A $(0,2)$ singlet was prepared at point P, off the detuning axis, through rapid relaxation to the ground state, then moved to the separation point S in $(1,1)$. Uncorrelated Overhauser fields in the two dots create an evolving Zeeman gradient, ΔB_z , that drives transitions between S and T_0 . Single-shot readout was performed by moving to point M, where S can tunnel to $(0,2)$ while T_0 remains in $(1,1)$. The reflectometer signal was integrated for 600 ns per shot, averaged over 10^4 shots, and compared to voltage values corresponding to S and T_0 outcomes [25], yielding $P_S(\tau_D)$, the probability of singlet return.

Coherence lost due to (thermally driven) evolution of ΔB_z can be partially restored using a Hahn echo by pulsing at time $\tau_D/2$ to point E, where the exchange splitting between S and T_0 drives a π -rotation about the \hat{x} axis, changing the sign of the acquired phase. Returning to S for an equal time $\tau_D/2$ cancels the phase acquired due to the low-frequency ($\omega < 2/\tau_D$) end of the spectrum of fluctuations of ΔB_z [11, 12]. Dynamical decoupling using a series of π -pulses allows efficient removal of more of the low-frequency end of the noise spectrum [11, 12]. The CPMG sequence [26], for example, uses evenly spaced gate pulses from point S to point E with a half interval before the first and after the last π -pulse [Figs. 2(b,c)]. Concatenated dynamical decoupling [9] (CDD) uses nonuniformly spaced pulses to point E, where the k -th order sequence is determined recursively from the lower order one, with an additional π -pulse in the center of odd orders [Fig. 2(d)].

Singlet return probabilities $P_S(\tau_D)$ were measured for CPMG sequences with $n_\pi = 1, 2, 3, 4, 8, 16$, and 32 . Fits to $P_S = 0.5 + V/2 \exp[-(\tau_D/T_2)^\alpha]$, with visibility V , T_2 , and α as a fit parameter, were equally good for α between 2 and 4, as seen in Fig. 3(a). For this reason, though $S(\omega)$ is related to α , these fits give little information about the spectrum of the environment. Figure

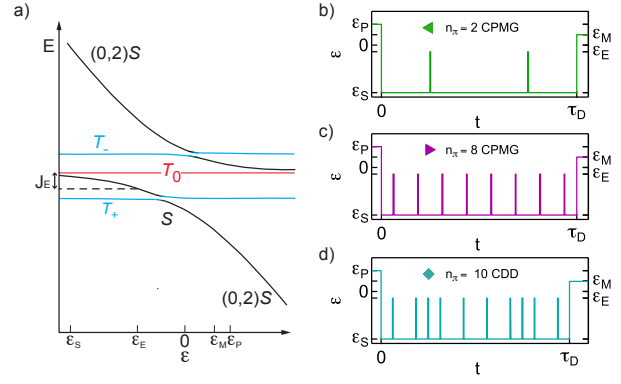


FIG. 2: (Color online) (a) Energy level diagram along the detuning axis ϵ . The $(0,2)$ singlet was prepared at ϵ_P , followed by separation to ϵ_S . π -pulses are performed at ϵ_E , allowing for subsequent rephasing at ϵ_S . Single-shot readout at ϵ_M using a proximal sensor dot. The exchange energy, J_E , that drives the π -pulses at ϵ_E is indicated by a dashed line. (b-d) Schematics of detunings during CPMG and CDD pulse sequences with detuning points on the vertical axis.

3(b), showing T_2 as a function of n_π for an even number of CPMG pulses, shows two remarkable features. First, values of T_2 do not depend on the value of α used in the fits to $P_S(\tau_D)$. Second, T_2 shows a power-law scaling $T_2 = T_2^0(n_\pi)^\gamma$ whose power, γ , also does not depend on the value of α used in the fits.

To model these observations, we consider Gaussian noise affecting the energy splitting of the qubit, which leads to the off-diagonal (in the basis of $|\uparrow\downarrow\rangle$ and $|\downarrow\uparrow\rangle$) elements of the qubit density matrix decaying as $\exp[-\chi(\tau_D)]$, where

$$\chi(\tau_D) = \int_0^\infty \frac{d\omega}{\pi} S(\omega) \frac{F(\omega\tau_D)}{\omega^2}, \quad (1)$$

with $F(\omega\tau_D)$ being the filter function determined by the sequence of π -pulses driving the qubit. For CPMG sequence $F(z) < (z/2n_\pi)^4$ for $z < 2n_\pi$, i.e. $F(z)$ strongly suppresses the low-frequency noise, while for large z and n_π the filter function can be approximated [12] by a periodic train (with period $z_p = 2\pi n_\pi$) of square peaks of height $h \approx 2n_\pi^2$ and width $\Delta z \approx z_p^2/\pi h \ll z_p$.

We find that the value of γ_e and the presence of an even-odd effect (EOE) in n_π (i.e. $\gamma_e \neq \gamma_o$) act as discriminators for several classes of $S(\omega)$: (i) The case of $0 < \gamma_e \leq 2/3$ and absent EOE is compatible with a model of $S(\omega) \sim \omega^{-\beta}$ (over a range of ω roughly bounded by the minimal and maximal values of n_π/τ_D), with $0 < \beta \leq 2$. In this case $\gamma_e = \beta/(1 + \beta)$ and $\alpha = \beta + 1$. One example is the case of Ornstein-Uhlenbeck noise [28] (having Lorentzian $S(\omega)$ with ω^{-2} tail typically dominating the decoherence under dynamical decoupling), where $\gamma = 2/3$ was confirmed by experiments on the NV center [4]. (ii) When an EOE is present, $\gamma_e = 2/3$ suggests a hard cut-

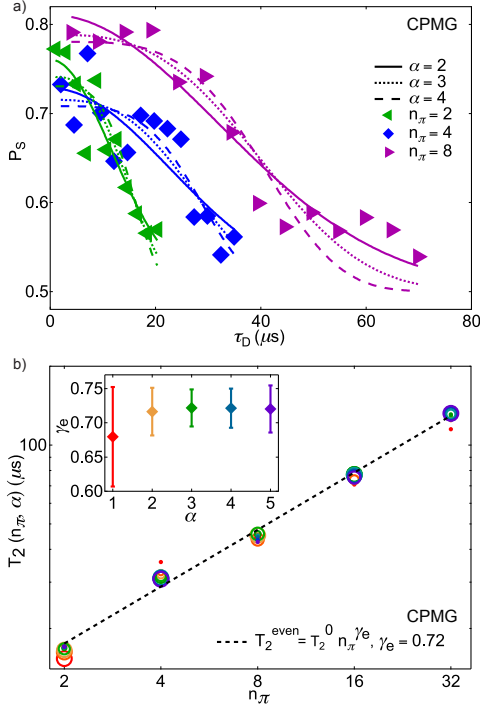


FIG. 3: (Color online) (a) Experimental singlet return probabilities as a function of time for CPMG with $n_\pi = 2, 4, 8$. Fits to $P_S(\tau_D) = 0.5 + V/2 \exp(-(\tau_D/T_2)^\alpha)$, with α constrained to 2 (solid curves), 3 (dotted curves) and 4 (dashed curves) [27]. It is difficult to determine α from these fits. (b) Extracted T_2 for even- n_π CPMG sequences for α constrained to 1, 2, 3, 4, and 5. Circle size proportional to χ^2 goodness of fit of $P_S(\tau_D)$ in (a). A power-law fit to the form $\ln(T_2^{\text{even}}(\alpha)) = \ln(T_2^0) + \gamma_e \ln(n_\pi)$, shown for $\alpha=3$ (dashed line) gives $\gamma_e = 0.72$. The fit value γ_e depends only weakly on α in the range 2 – 5 (inset). The weighted average over $\alpha = 2 - 5$ yields $\gamma_e = 0.72 \pm 0.01$.

off in $S(\omega)$ at $\omega_c < 2/T_2$, in which case $\gamma_o = 1$. (iii) For $\omega_c > 2/T_2$, i.e. for larger ω_c or larger n_π (leading to longer T_2), the EOE disappears and γ tends to 1 [14]. (iv) Finally, the presence of the EOE and $2/3 < \gamma_e < 1$ indicate $S(\omega) \sim \omega^{-\beta}$, with $\beta > 2$.

Experimentally, we find $\gamma_e = 0.72$ for even number of CPMG pulses, and $n_\pi = 1$ not along the scaling line, indicating an EOE. We conclude that scenario (iv) applies, namely $S(\omega) = A^{\beta+1}/\omega^\beta$ with $2 < \beta < 3$. Using Eq. (1) and the CPMG filter function gives in the large- n_π limit

$$\chi(t) \approx (A\tau_D)^{1+\beta} \left(\frac{a}{n_\pi^\beta} + \frac{b_{e/o}}{n_\pi^4} \right), \quad (2)$$

with $a \approx \Sigma_{2+\beta}/\pi^2(2\pi)^\beta$, where $\Sigma_\delta = \sum_{k=1}^\infty (k - \frac{1}{2})^{-\delta}$, and for odd (even) n_π we have $b_o \approx [32\pi(3 - \beta)]^{-1}$ ($b_e \approx [128\pi(5 - \beta)]^{-1} \approx b_o/10$), i.e., the b/n_π^4 term is negligible for even n_π , while it gives a significant correction for small, odd n_π . The EOE comes from the difference in the low- z behavior of the CPMG filter functions, which for $z < 1$ behave as $F(z) \sim z^4/2^5 n_\pi^4 (z^6/2^7 n_\pi^4)$ for odd

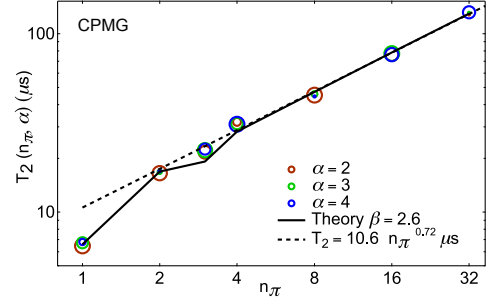


FIG. 4: (Color online) T_2 for all measured n_π for CPMG, extracted using $\alpha = 2, 3$, and 4 (circles). Circle size for each α proportional to χ^2 goodness of fit. Theory (black solid curve) for $\beta = \gamma_e/(1 - \gamma_e) = 2.6$ and integration of Eq. (1) with the CPMG filter functions. Note that Eq. (2) captures the even/odd effect quantitatively for small n_π .

(even) n_π . For $\beta > 2$ this leads to different contributions of very low ω to the integral in Eq. (1). For even n_π , we find that $\chi(\tau_D)$ approximately reduces to $(A\tau_D)^{1+\beta} a/n_\pi^\beta$, from which we obtain the $\beta \leq 2$ result of $\gamma_e = \beta/(1 + \beta)$ in this case as well.

Assuming this form of $S(\omega)$, fits to the even n_π [Fig. 3(b)] yield $\beta = 2.6$ and $A^{-1} = 3.6 \mu\text{s}$. Using these two parameters we calculate odd- n_π values for T_2 by numerically integrating Eq. (1). As shown in Fig. 4, the obtained value of T_2 is in good agreement with the measured value for $n_\pi = 1$ (Hahn echo). We note that the large n_π scaling of $T_2 \sim n_\pi^\gamma$ is due to the behavior of $S(\omega)$ at $\omega \geq \pi n_\pi/T_2$, which is $\sim 0.3(n_\pi)^{0.28} \mu\text{s}^{-1}$ here, while the EOE at small n_π is due to behavior at $\omega < 1/T_2$, which is $\sim 0.15 \mu\text{s}^{-1}$. The consistency between small- and large- n_π data indicates that $S(\omega) \sim \omega^{-2.6}$ over this range of frequencies (i.e., $\omega/2\pi \sim 10 - 100 \text{ kHz}$). The EOE behavior at low n_π can be fit within scenario (ii) using $S(\omega) = A^3/\omega^2$ with $A^{-1} \sim 1 \mu\text{s}$ and $\omega_c \sim 0.08 \mu\text{s}^{-1}$. However, this scenario crosses over to (iii) for $n_\pi > 5$, where γ tends to 1. The resulting large- n_π behavior, $T_2 \sim n_\pi \times 7 \mu\text{s}$, departs significantly from the $n_\pi \geq 8$ data in Fig. 4.

Using $S(\omega) = A^{\beta+1}/\omega^\beta$ with parameters A and β fixed from the even- n_π CPMG fit, we can calculate the expected dependence of $T_2(n_\pi)$ for the CDD pulse sequence using the known filter functions [12]. For $n_\pi = 5, 10$, and 21 we get good agreement between the calculated and measured T_2 [Fig. 5]. For $n_\pi = 42$, the experimental T_2 is shorter than predicted by theory, possibly reflecting an accumulation of errors for such a large number of pulses. Note that CDD was shown to be robust to pulse errors [29] only in the case of two-axis control (i.e. when the π -pulses are about x and y axes alternately) and for a quasi-static bath.

Summarizing, the measurements of qubit decoherence under dynamical decoupling with the CPMG pulse sequence have been used to reconstruct the crucial features

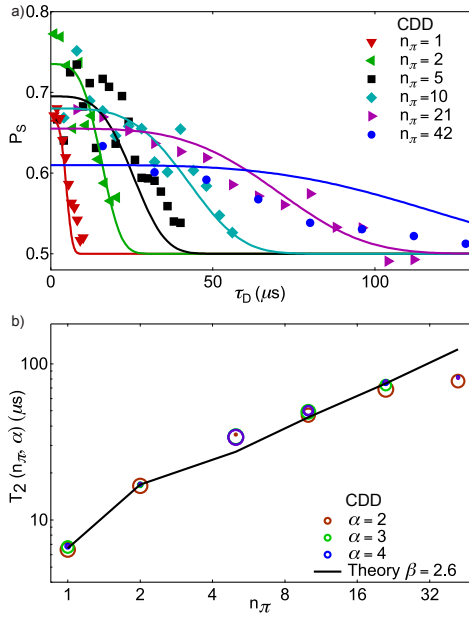


FIG. 5: (Color online) (a) Experimental singlet return probabilities for orders 1 through 6 CDD (symbols) along with fits to $P_S(\tau_D) = 0.5 + V/2 \exp(-(\tau_D/T_2)^\alpha)$ using $\beta = \gamma_e/(1 - \gamma_e) = 2.6$ (solid curves). (b) Extracted T_2 for using different values of α (circle size proportional to χ^2 measure of goodness of fit). Theory (solid curve) based on $\beta = \gamma_e/(1 - \gamma_e) = 2.6$ and integration of Eq. (1) with appropriate CDD filter function [12].

of the spectral density of noise dephasing the qubit. Using the data for even n_π of CPMG we have been able to estimate the magnitude of noise and its functional form. The reconstructed spectral density of noise allows us to calculate the expected decoherence signal for other pulse sequences, and this calculation agrees with the CDD sequence measurements for n_π as well as the odd- n_π CPMG data. We have shown that instead of fitting the exact functional form of the coherence decay function, an analysis of the scaling of the measured T_2 time with the number of applied pulses allows for a clearer understanding of the system. We cannot say at this point whether the observed value $\gamma_e = 0.72$ is characteristic of Overhauser-dominated dephasing in general, or just our particular combination of noise sources.

We acknowledge funding from IARPA under the MQCO program, from NSF under the Materials World Network program, and from the Homing Programme of the Foundation for Polish Science supported by the EEA Financial Mechanism (LC). We thank M. Biercuk and V. Dobrovitski for useful discussions.

[1] H. Bluhm, S. Foletti, I. Neder, M. Rudner, D. Mahalu, V. Umansky, and A. Yacoby, Nat. Phys. **7**, 109 (2011).

[2] C. Barthel, J. Medford, C. M. Marcus, M. P. Hanson, and A. C. Gossard, Phys. Rev. Lett. **105**, 266808 (2010).
[3] J. Bylander, S. Gustavsson, F. Yan, F. Yoshihara, K. Harrabi, G. Fitch, D. G. Cory, Y. Nakamura, J.-S. Tsai, and W. D. Oliver, Nat. Phys., advance online publication (2011).
[4] G. de Lange, Z. H. Wang, D. Ristè, V. V. Dobrovitski, and R. Hanson, Science **330**, 60 (2010).
[5] M. J. Biercuk, H. Uys, A. P. VanDevender, N. Shiga, W. M. Itano, and J. J. Bollinger, Nature **458**, 996 (2009).
[6] Y. Sagi, I. Almog, and N. Davidson, Phys. Rev. Lett. **105**, 053201 (2010).
[7] L. Viola and S. Lloyd, Phys. Rev. A **58**, 2733 (1998).
[8] G. S. Uhrig, Phys. Rev. Lett. **98**, 100504 (2007).
[9] K. Khodjasteh and D. A. Lidar, Phys. Rev. A **75**, 062310 (2007).
[10] K. Khodjasteh, T. Erdélyi, and L. Viola, Phys. Rev. A **83**, 020305 (2011).
[11] R. de Sousa, Top. Appl. Phys. **115**, 183 (2009).
[12] L. Cywiński, R. M. Lutchyn, C. P. Nave, and S. Das Sarma, Phys. Rev. B **77**, 174509 (2008).
[13] M. J. Biercuk, A. C. Doherty, and H. Uys, J. Phys. B: At. Mol. Opt. Phys. **44**, 154002 (2011).
[14] M. J. Biercuk and H. Bluhm, Phys. Rev. B **83**, 235316 (2011).
[15] W. Yao, R.-B. Liu, and L. J. Sham, Phys. Rev. B **74**, 195301 (2006).
[16] W. M. Witzel and S. Das Sarma, Phys. Rev. B **74**, 035322 (2006).
[17] W. M. Witzel and S. Das Sarma, Phys. Rev. Lett. **98**, 077601 (2007).
[18] L. Cywiński, W. M. Witzel, and S. Das Sarma, Phys. Rev. B **79**, 245314 (2009).
[19] I. Neder, M. S. Rudner, H. Bluhm, S. Foletti, B. I. Halperin, and A. Yacoby, Phys. Rev. B **72**, 052113 (2011).
[20] G. Gordon, G. Kurizki, and D. A. Lidar, Phys. Rev. Lett. **101**, 010403 (2008).
[21] Y. Pan, Z.-R. Xi, and W. Cui, Phys. Rev. A **81**, 022309 (2010).
[22] A. Ajoy, G. A. Álvarez, and D. Suter, Phys. Rev. A **83**, 032303 (2011).
[23] D. J. Reilly, C. M. Marcus, M. P. Hanson, and A. C. Gossard, Appl. Phys. Lett. **91**, 162101 (2007).
[24] C. Barthel, M. Kjærgaard, J. Medford, M. Stopa, C. M. Marcus, M. P. Hanson, and A. C. Gossard, Phys. Rev. B **81**, 161308 (R) (2010).
[25] C. Barthel, D. J. Reilly, C. M. Marcus, M. P. Hanson, and A. C. Gossard, Phys. Rev. Lett. **103**, 160503 (2009).
[26] L. M. K. Vandersypen and I. L. Chuang, Rev. Mod. Phys. **76**, 1037 (2005).
[27] CPMG visibilities for $\alpha = 2$ are: $n_\pi = 2, V = 0.52 \pm 0.02$; $n_\pi = 4, V = 0.46 \pm 0.04$; $n_\pi = 8, V = 0.62 \pm 0.02$. Visibilities for $\alpha = 3$ are: $n_\pi = 2, V = 0.48 \pm 0.03$; $n_\pi = 4, V = 0.43 \pm 0.02$; $n_\pi = 8, V = 0.58 \pm 0.03$. Visibilities for $\alpha = 4$ are: $n_\pi = 2, V = 0.46 \pm 0.03$; $n_\pi = 4, V = 0.42 \pm 0.02$; $n_\pi = 8, V = 0.56 \pm 0.03$.
[28] V. V. Dobrovitski, A. E. Feiguin, R. Hanson, and D. D. Awschalom, Phys. Rev. Lett. **102**, 237601 (2009).
[29] Z.-H. Wang, W. Zhang, A. M. Tyryshkin, S. A. Lyon, J. W. Ager, E. E. Haller, and V. V. Dobrovitski, arXiv:1011.6417 (2010).